

On the Stability of Robotic Systems Worn by Humans

H. Kazerooni, J. Douglas Meidt

Mechanical Engineering Department
University of Minnesota
Minneapolis, MN 55455

ABSTRACT

An extender is defined to be an active manipulator worn by a human to increase his strength [6]. The human, in physical contact with the extender, exchanges power and information signals with the extender. The human arm, the extender, and the environment comprise the dynamic model of the extender system. In this paper, an expression for system performance is derived to determine the force augmentation of the extender. The stability and the performance of the extender are proven via simulation and via experiments with a single-degree-of-freedom hydraulic extender. The trade-off between performance and stability is discussed: the better the required performance (larger force amplification in this experiment), the narrower the stability range is.

1. INTRODUCTION

A robot manipulator's performance of physical tasks depends on its actuator torque: a small actuator can supply a large torque. Human performance of physical tasks is limited, not by human intelligence, but by human physical strength. However, human mechanical power can be integrated with robot mechanical power under the control of the human intellect in the class of robot manipulators called "extenders". Extenders use actuator power to extend human strength while maintaining human control of the task. The human wears the extender on his arm and feels a scaled-down version of the load carried by the extender. Such physical contact allows direct transfer of information signals and mechanical power between the human and the extender. This direct transfer distinguishes the extender from conventional master-slave systems because control of the extender trajectory can be accomplished without a joystick, keyboard, or other master-slave device. Instead, input to the extender is derived from the human-extender contact forces which are measured, modified to satisfy performance and stability criteria, and fed to the extender controller.

The concept of a device to increase the strength of a human operator using a master-slave system has existed since the early 1960s and was originally named "man-amplifier" [1,2,3,4,12,14,15,16,17]. The man-amplifier was defined as a manipulator which would greatly increase the strength of a human operator while maintaining human control of the manipulator. These early systems were based upon the master-slave concept rather than upon direct physical contact between human and manipulator.

An experimental extender is shown in Figure 1a. The human arm, wrapped in a cylinder of rubber for a snug fit, is located in the inner tube. A piezoelectric load cell, placed between the tubes, measures the interaction force between the human arm and the extender. Another piezoelectric force cell, set between the extender and the environment, measures the interaction force between the extender and the environment. A rotary hydraulic actuator, mounted on a solid platform, powers the outer tube of the extender. The actuator shaft, supported by two bearings, is connected to the outer tube to transfer power.

This article establishes experimentally-verified ground rules for control of human-machine interaction in the sense of transfer of power and information signals. Human-extender interaction and its dynamic behavior are described. A mathematical description of extender performance is derived. The stability of the human-extender-load system is analyzed. The trade-offs between performance and stability are examined.

2. DYNAMIC BEHAVIOR OF THE EXTENDER

If an extender has elements with significant dynamic behavior, such as hydraulic actuators or transmission systems, rigid-body dynamics [5] can not sufficiently represent the extender dynamic behavior. In the modeling approach taken here, the dynamics of the extender elements are implicitly included in an unstructured model by focusing on the input and output properties of the extender.

The extender position, y_e , is an $n \times 1$ function of two variables: the electronic command to the extender drive system and the external forces imposed on the extender. It is assumed that the extender has either a closed-loop velocity or closed-loop position controller. This controller, called a primary stabilizing compensator in this article, is chosen because the extender must be stable when no one is wearing it and because robustness in the extender can be created without considering human and object dynamics.

Regardless of the type of primary stabilizing compensator, it is assumed that the extender position y_e is the extender model output, u_e is the input electronic command to the primary compensator¹, f_{eh} is the force imposed by the human on the extender, and f_{eo} is the

¹ If the primary compensator is a position controller, then u_e is the position reference and y_e follows u_e according to the employed control law. If the primary compensator is a velocity controller, then \dot{y}_e , the extender velocity, follows u_e according to the employed control law.

force imposed by the environment (the object being manipulated) on the extender. The following equation summarizes the extender dynamic behavior:

$$y_e = E_x(u_e, f_{eh}, f_{en}) \quad (1)$$

If a position controller is selected to be the primary stabilizing compensator, mapping 1 is stable. However, if a velocity controller is selected to be the primary controller, the extender position is not a stable function of the extender inputs. The following norm inequality can be defined by taking the truncated L_2 norms of both sides of equation 1:

$$\|y_{e,T}\|_2 < \alpha_{ue} \|u_{e,T}\|_2 + \alpha_{feh} \|f_{eh,T}\|_2 + \alpha_{fen} \|f_{en,T}\|_2 + \beta_{ye} \quad \forall t \in T \quad (2)$$

where α_{ue} , α_{feh} , α_{fen} , and β_{ye} are positive constants and $y_{e,T}$, $u_{e,T}$, $f_{eh,T}$, and $f_{en,T}$ are the truncated functions².

3. DYNAMIC BEHAVIOR OF THE HUMAN ARM

The behavior of the human arm is modeled here as a relationship between inputs and outputs so that the dynamics of nerve conduction, muscle contraction, and central nervous system (CNS) processing are implicitly considered. The focus is on constrained maneuvers of the extender in which the environment continuously exerts a dynamic constraint on the extender and thus on the human arm. No particular type of control action (force or velocity or position) is attributed to the arm since it is not certain which of these types is commanded by the CNS. Thus, to arrive at a general model for the human-extender dynamic behavior, a Norton equivalent concept is used. Modeling the human arm with such an equivalent does not affect the arm's interaction with other systems.

The Norton equivalent models the human arm dynamic behavior as a non-ideal source of force interacting with other systems. "Non-ideal" indicates the arm responds both to position disturbances from the extender and to force commands from the CNS. The force between the extender and arm results from two inputs: u_h , issued by the CNS, and extender motion (position and/or velocity), if such motion occurs. u_h is human thought deciding to impose the force of f_{eh} . S_h , which represents the disturbance rejection property of the human arm, maps y_e into f_{eh} . The following equation represents the human arm dynamic behavior:

$$f_{eh} = u_h - S_h(y_e) \quad (3)$$

Since it is assumed that the human arm is stable, the following norm inequality can be defined by taking the L_2 norms of both sides of equations 3:

$$\|f_{eh}\|_2 < \|u_h\|_2 + \alpha_{sh} \|y_e\|_2 + \beta_{feh} \quad (4)$$

where α_{sh} and β_{feh} are positive constants.

4. DYNAMIC BEHAVIOR OF THE ENVIRONMENT

The extender can either manipulate heavy objects or impose large forces on objects. Figure 1a shows a single-degree-of-freedom prototype extender pushing against a compliant element. If the

positive direction of f_{en} is defined to be from the environment to the extender, the constraining force of $-[C\dot{y}_e + K y_e]$, where y_e is the extender position, is imposed on the extender.

If E_n , a nonlinear operator, is the environment dynamics, and f_{ext} is all external forces on the environment, a general expression for f_{en} as a function of y_e is:

$$f_{en} = f_{ext} - E_n(y_e) \quad (5)$$

It is not clear if the environment is an L_2 stable function of y_e . Similar to the extender dynamic behavior, mapping 5 is assumed to be bounded within any bounded interval T . The following norm inequality can be defined by taking the L_2 norms of both sides of equation 5:

$$\|f_{en,T}\|_2 < \alpha_{En} \|y_{e,T}\|_2 + \|f_{ext,T}\|_2 + \beta_{fen} \quad \forall t \in T \quad (6)$$

where α_{En} and β_{fen} are positive constants.

In the example of Figure 1a, E_n is equal to the environment impedance $(K + Cs)$. Figure 1b shows another example where the extender is manipulating mass m with acceleration \ddot{y}_e . If the direction of f_{en} is defined as from the environment to the extender, the constraining clockwise torque of $[m l_{en}^2 \ddot{y}_e + m g l_{en} \cos(y_e)]$, where y_e is the angular orientation of the extender, is imposed on the extender. $E_n(\cdot)$ in this example is a nonlinear function such that $E_n(y_e) = [m l_{en}^2 \ddot{y}_e + m g l_{en} \cos(y_e)]$ and $f_{ext} = 0$.

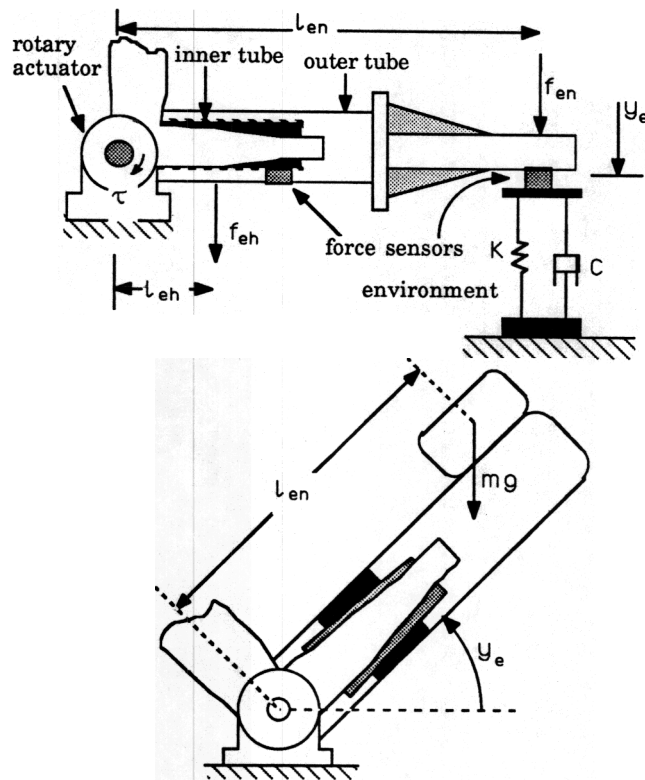


Figure 1: a: The force imposed on the extender from the environment is an upward force of $-(K + Cs)y_e$. b: The torque that constrains the extender motion in a free maneuver is a clockwise torque of $[m l_{en}^2 \ddot{y}_e + m g l_{en} \cos(y_e)]$

5. DYNAMIC MODEL OF THE EXTENDER, HUMAN, AND ENVIRONMENT

The total dynamic behavior of the extender, human, and environment is shown in Figure 2. If u_e , u_h , and f_{ext} are zero, f_{en} is zero. If u_h alone takes on a nonzero value because the human decides to move his hand, then an extender motion develops from

² If $\|y_e\|_2 < \infty$, then $y_e \in L_2$, which implies that y_e is L_2 -stable. In cases where the norm may approach infinity, a truncated function $y_{e,T}$ is defined as:

$$y_{e,T} = y_e, \quad t \leq T$$

$$y_{e,T} = 0, \quad t > T$$

If $\|y_{e,T}\|_2 < \infty$, then y_e belongs to the extended L_2 -space denoted by L_2^e . This definition facilitates the analysis of systems in which the subsystems are unstable while the entire system may be stable. Although mapping 1 may not be L_2 stable, inequality 2 assumes that within any limited time, T , the extender position will be bounded whether the extender primary controller is a position controller or a velocity controller.

f_{eh} . This motion may be small if α_{feh} is small even if f_{eh} is large: the human arm may not have the strength to overcome the extender primary closed-loop control. To increase the human's effective strength, the extender's apparent sensitivity is increased by measuring f_{eh} and filtering it through the compensator H_1 . The compensator output is an input command u_e to the extender. Similarly, compensator H_2 generates extender compliancy in response to f_{en} . H_1 and H_2 must be chosen to ensure stability for the closed-loop system.

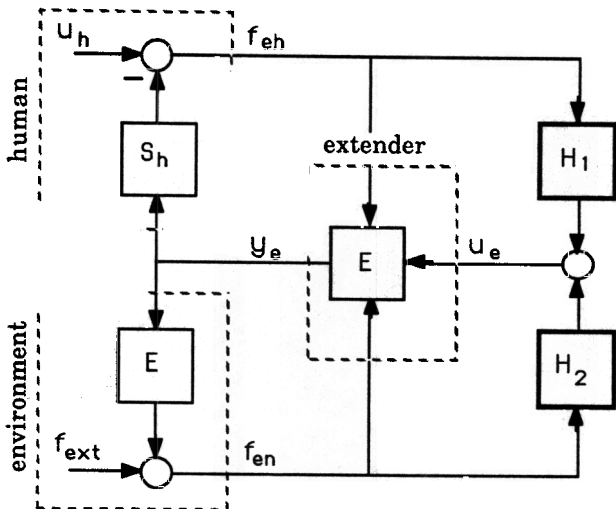


Figure 2: Compensators H_1 and H_2 increase the apparent sensitivity of the extender to forces from the human and from the environment.

6. PERFORMANCE

This section addresses the following question: What dynamic behavior should the extender have in performing a task? The resulting performance specification does not assure the stability of the system in Figure 2 but does let designers express what they wish to have happen during a maneuver if instability does not occur. (Section 8 shows that designers must accept a trade-off between performance and closed-loop stability.) The following example describes a performance specification for the extender. Suppose the extender is employed to manipulate an object through a completely arbitrary trajectory³. It is reasonable to ask for an extender dynamic behavior where the human feels the scaled-down values of the forces on the extender: that is, the human has a natural sensation of the forces required to maneuver the load. In other words, the human would feel the scaled-down values of the acceleration, centrifugal, coriolis, and gravitational forces associated with an arbitrary maneuver. This example calls for masking the dynamic behavior of the extender, human, and load via the design of H_1 and H_2 such that a desired relationship is guaranteed between f_{eh} and f_{en} . Without any proof, it is stated that only two relationships among f_{eh} , f_{en} , and u_e are needed to specify a unique behavior for the extender. If two relationships, one between f_{en} and f_{eh} and one between f_{eh} and u_e , are specified, then the relationship between f_{en} and u_e cannot be specified. Therefore, the objective is to choose H_1 and H_2 so that two independent relationships can be established among f_{eh} , f_{en} , and u_e . The following equations are suggested as the two target relationships:

$$f_{eh} = P(f_{en})$$

$$f_{eh} = R(u_e) \tag{8}$$

³ For clarity in understanding the concept of performance, it is assumed that f_{ext} on the object is zero. The equations derived in this section can be extended to cases where f_{ext} is not zero.

$P(\cdot)$ and $R(\cdot)$ are arbitrary nonlinear target dynamics. The first equation, which is the most natural design specification for extenders, allows the designers to specify a relationship between the forces f_{eh} and f_{en} . The second relationship establishes an impedance for the extender. The following describes two design examples in which only one design specification is of interest.

I. Shaping the Force

Suppose the purpose is to guarantee a relationship between the forces f_{eh} and f_{en} (equation 7) without concern for the relationship between f_{eh} and u_e (equation 8). Since only one relationship is specified, there may be infinite choices for H_1 and H_2 . The choice suggested here ensures ease of implementation. (Refer to experiments for a discussion on implementation.) A trajectory controller can be designed so that α_{fen} and α_{feh} are small gains and E_x creates an approximately unity gain from u_e to y_e . This can be achieved by implementing a position controller that creates a large open-loop gain in the system. For example, if several integrators are used in the extender primary controller, then α_{feh} and α_{fen} are small which results in small extender response to f_{eh} and f_{en} . The governing dynamic equation when the primary controller is insensitive to f_{eh} and f_{en} is:

$$u_e \approx H_1(f_{eh}) + H_2(f_{en}) \tag{9}$$

H_1 and H_2 are chosen as:

$$H_1(f_{eh}) = 2 E_n^{-1} [-P^{-1}(f_{eh})] \tag{10}$$

$$H_2(f_{en}) = -E_n^{-1} (-f_{en}) \tag{11}$$

$E_n^{-1}(-f_{en})$ is the solution of the environment dynamic equation for a given $-f_{en}$; u_e must be calculated from equation 5 for any given $-f_{en}$. Substituting H_1 and H_2 (equations 10 and 11) into equation 9 results in equation 12.

$$u_e \approx -E_n^{-1} (-f_{en}) + 2 E_n^{-1} [-P^{-1}(f_{eh})] \tag{12}$$

Since $u_e = E_n^{-1}(-f_{en})$, then:

$$E_n^{-1}(-f_{en}) \approx -E_n^{-1} (-f_{en}) + 2 E_n^{-1} [-P^{-1}(f_{eh})] \tag{13}$$

and, consequently:

$$f_{eh} \approx P(f_{en}). \tag{14}$$

In an example illustrating the above case, an extender is used to hold a jackhammer. The objective is to decrease and filter the force transferred to the human arm so the human feels only the low-frequency force components. This requires that $f_{eh} = -\alpha M(s) f_{en}$ where, preferably, $M(s)$ is a diagonal matrix with low-pass filter transfer functions as members. α is a scalar smaller than unity and represents the force reduction. Choosing $P(s) = -\alpha M(s)$, the required forms of H_1 and H_2 are as follows:

$$H_1(f_{eh}) = 2 E_n^{-1} \left\{ \frac{1}{\alpha} M^{-1}(s) f_{eh} \right\} \tag{15}$$

$$H_2(f_{en}) = -E_n^{-1} (-f_{en}) \tag{16}$$

Substituting H_1 and H_2 from equations 15 and 16 into equation 9 results in $f_{eh} \approx -\alpha M(s) f_{en}$. The above method calls for the class of P functions that are exactly invertible or at least can be inverted approximately. For example, if $M(s)$ is chosen as a first-order filter, then $M^{-1}(s)$ in equation 15 can be realized for a bounded frequency range.

II. Shaping the Impedance

Suppose the purpose is to guarantee a relationship between the forces f_{eh} and u_e (equation 8) without any regard to the relationship between f_{eh} and f_{en} . Again, a trajectory controller can be designed so that α_{fen} and α_{feh} have very small gains and E_x creates an approximate unity gain from u_e to y_e . Therefore, equation 9 governs

one of the

the dynamic behavior of the system. Suppose H_1 and H_2 are chosen such that:

$$H_1(f_{eh}) = 2 R^{-1}(f_{eh}) \quad (17)$$

$$H_2(f_{en}) = -E_n^{-1}(-f_{en}) \quad (18)$$

Substituting H_1 and H_2 from equations 17 and 18 into equation 9 results in equation 19.

$$y_e \approx -E_n^{-1}(-f_{en}) + 2 R^{-1}(f_{eh}) \quad (19)$$

Since $y_e = E_n^{-1}(-f_{en})$, then equation 19 results in equation 20.

$$y_e \approx R^{-1}(f_{eh}) \quad (20)$$

Equation 20 guarantees that the target impedance in equation 8 has been achieved.

In an example for this case, the goal is to feel the forces resulting from maneuvering a point mass when maneuvering a rigid body. This behavior requires masking the cross-coupled forces associated with rigid body maneuvers. This behavior is characterized by $f_{eh} = D(s)y_e$ where $D(s)$ is a diagonal matrix with second-order functions as members and s is the Laplace operator. For a two dimensional maneuver, $D(s)$ is shown in equation 21 where m_1 and m_2 are chosen to be the "apparent masses" in two directions.

$$D(s) = \begin{pmatrix} m_1 s^2 & 0 \\ 0 & m_2 s^2 \end{pmatrix} \quad (21)$$

Equation 21 guarantees a natural sensation of the forces used to maneuver a point mass. Choosing $H_1(s) = 2 D^{-1}(s)$ and $H_2(f_{en}) = -E_n^{-1}(-f_{en})$ and substituting them in equation 9 results in $f_{eh} \approx D(s)y_e$.

7. CLOSED-LOOP STABILITY

A sufficient condition for stability of the closed-loop system of Figure 2 is developed by the Small Gain Theorem. This sufficient condition results in a class of compensators which guarantee the stability of the closed-loop system in Figure 2. Note that the stability condition derived in this section does not give any indication of system performance, but only ensures a stable system. This stability condition also clarifies the trade-off between performance and closed-loop stability. (Refer to reference 17 to understand the mathematical notation used in this analysis.) Suppose H_1 and H_2 are chosen as nonlinear operators such that $H_1, H_2: L^{\infty}_{2e} \rightarrow L^{\infty}_{2e}$ and:

$$\|H_1(f_{eh,T})\|_2 < \alpha_{H1} \|f_{eh,T}\|_2 + \beta_{H1} \quad (22)$$

$$\|H_2(f_{en,T})\|_2 < \alpha_{H2} \|f_{en,T}\|_2 + \beta_{H2} \quad (23)$$

where α_{H1} , α_{H2} , β_{H1} and β_{H2} are positive constants. Since $u_e = H_1(f_{eh}) + H_2(f_{en})$:

$$\|u_{e,T}\|_{\infty} < \alpha_{H1} \|f_{eh,T}\|_2 + \alpha_{H2} \|f_{en,T}\|_2 + \beta_{H1} + \beta_{H2} \quad (24)$$

Substituting $\|f_{eh,T}\|_2$, $\|f_{en,T}\|_2$, $\|u_{e,T}\|_2$ from inequalities 4, 6, and 24 into inequality 2 results in inequality 25 for $\|y_e\|_2$:

$$\begin{aligned} \|y_{e,T}\|_2 &< (\alpha_{feh} \alpha_{sh} + \alpha_{fen} \alpha_{En} + \alpha_{ue} \alpha_{H1} \alpha_{sh} + \alpha_{ue} \alpha_{H2} \alpha_{En}) \\ \|y_{e,T}\|_2 &+ (\alpha_{H1} \alpha_{ue} + \alpha_{feh}) \|u_{h,T}\|_2 + (\alpha_{H2} \alpha_{ue} + \alpha_{fen}) \\ \|f_{ext,T}\|_2 &+ (\alpha_{feh} + \alpha_{ue} \alpha_{H1}) \beta_{feh} + (\alpha_{fen} + \alpha_{ue} \alpha_{H2}) \beta_{fen} + \\ &\alpha_{ue} (\beta_{H1} + \beta_{H2}) + \beta_{ye} \end{aligned} \quad (25)$$

Employing the Small Gain Theorem, the closed-loop system of Figure 2 is L_2 stable if:

$$\alpha_{feh} \alpha_{sh} + \alpha_{fen} \alpha_{En} + \alpha_{ue} \alpha_{H1} \alpha_{sh} + \alpha_{ue} \alpha_{H2} \alpha_{En} < 1 \quad (26)$$

Inequality 26 expresses the stability condition of the closed-loop system in Figure 2. By inspection of inequality 26, it can be observed that the smaller H_1 and H_2 are, the larger the stability range is. To

illustrate the trade-off between stability and performance, a simple case is considered where a high gain positioning system is designed as the primary compensator such that α_{fen} and α_{feh} are rather small. The stability condition for small α_{fen} and α_{feh} reduces to:

$$\alpha_{ue} \alpha_{H1} \alpha_{sh} + \alpha_{ue} \alpha_{H2} \alpha_{En} < 1 \quad (27)$$

H_1 and H_2 represent the performance of the system. For example, when a larger H_1 is chosen for equation 15 (by choosing a smaller α), a larger torque amplification can be achieved. Designers, however, may not freely select H_1 : inequality 27 must also be guaranteed. If α_{En} is chosen to be zero, the stability condition applies to free maneuvers when the robot is not in contact with any object.

$$\alpha_{ue} \alpha_{H1} \alpha_{sh} < 1 \quad (28)$$

Inequality 28 states that guaranteeing stability of the closed-loop system requires some initial compliancy in the human arm. If the human hand has a large sensitivity to position disturbances (i.e.; it rejects position disturbances by moving very quickly), then the system stability can be guaranteed by a small H_1 . Large S_h implies a stiff human arm and, theoretically, as $\alpha_{sh} \rightarrow \infty$, the stability of the closed-loop system can no longer be guaranteed. More trade-offs between performance and stability are described in Section 9.

8. CLOSED-LOOP STABILITY (LINEAR ANALYSIS)

Using transfer function matrices, the linear dynamic behavior of the extender, human, and environment can be described by equations 29, 30 and 31.

$$y_e = G_e(s)u_e + S_{eh}(s)f_{eh} + S_{en}(s)f_{en} \quad (29)$$

$$f_{en}(s) = -E_n(s)y_e + f_{ext} \quad (30)$$

$$f_{eh} = -S_h(s)y_e + u_h \quad (31)$$

where G_e represents the closed-loop transfer function for the extender and S_{eh} and S_{en} represent the extender sensitivity transfer functions in response to forces f_{eh} and f_{en} . Using Multivariable Nyquist Theorem, inequality 32 can be used for the stability analysis [8,11].

$$\sigma_{\max}\{G_e H_1 S_h + G_e H_2 E_n\} < \sigma_{\min}\{I + S_{eh} S_h + S_{en} E_n\} \quad (32)$$

If a high gain positioning system is designed as the primary compensator for the extender, then S_{en} and S_{eh} are rather small and the stability condition reduces to:

$$\sigma_{\max}\{G_e H_1 S_h + G_e H_2 E_n\} < 1 \text{ for all } \omega \in [0, \infty) \quad (33)$$

Inequality 33 is similar to inequality 27. For a single-degree-of-freedom extender, the stability condition of 32 reduces to:

$$\left| \frac{G_e H_1 S_h + G_e H_2 E_n}{1 + S_{eh} S_h + S_{en} E_n} \right| < 1 \text{ for all } \omega \in [0, \infty) \quad (34)$$

If H_2 is chosen to be zero, then:

$$\left| H_1 \right| < \frac{1}{|G_e|} \left| S_{eh} + \frac{1}{S_h} + \frac{S_{en} E_n}{S_h} \right| \text{ for all } \omega \in [0, \infty) \quad (35)$$

If the extender is not in contact with any load ($E_n = 0$), the stability condition reduces to:

$$\left| H_1 \right| < \frac{1}{|G_e|} \left| S_{eh} + \frac{1}{S_h} \right| \text{ for all } \omega \in [0, \infty) \quad (36)$$

Inequality 36 states that, to guarantee the stability of the closed-loop system, there must be some initial compliancy in either the human arm, $1/S_h$, or the extender primary control system, S_{eh} . Loosely speaking, S_h represents the human hand stiffness. The system stability cannot be guaranteed if S_{eh} is very small (i.e., a stiff extender) and the human hand has infinite sensitivity to position disturbances (i.e., the human hand has a very large S_h and it does not reject position disturbances by moving very quickly). Inequality 36 also shows that the system has a smaller stability range when no load is in contact with the extender. Therefore, if the

extender is stable without any load, it is also stable for all possible values of the environment dynamics.

According to the results of section 6, the performance of the extender is determined by the chosen values of H_1 . The larger H_1 is chosen to be, the smaller the ratio of f_{eh} to f_{en} is. Loosely speaking, large H_1 allows the human to manipulate large objects or to impose large forces onto the environment. On the other hand, the stability conditions given above require small values for H_1 to guarantee the stability of the system. This trade-off between stability and performance is illustrated experimentally in the next section.

9. EXPERIMENTAL EXTENDER

A single-degree-of-freedom extender (Figure 1a) is used to verify experimentally the theoretical predictions for extender stability and performance. This experimental extender consists of an outer tube (39.5 lbf) and an inner tube. The human arm, wrapped in a cylinder of rubber for a snug fit, is located in the inner tube. A piezoelectric load cell, placed between these tubes, measures the interaction force between the human arm and the extender, f_{eh} . Another piezoelectric force cell, set between the extender and the environment, measures the interaction force between the extender and environment, f_{en} . A rotary hydraulic actuator, mounted on a solid platform, powers the outer tube of the extender. The actuator shaft, supported by two bearings, is connected to the outer tube to transfer power. In addition to the piezoelectric load cells, other sensing devices include a tachometer and an encoder (with a corresponding counter) to measure the angular speed and position of the motor shaft. An automobile strut, mounted on a custom fixture below the extender, is the experimental environment. An IBM/AT computer is used for data acquisition and control. Based on the information from these sensors, a control algorithm calculates a command signal which is sent to the extender servo controller board via a digital-to-analog (D/A) converter.

Figure 3 shows a position controller as the primary stabilizing controller for the extender. The closed-loop position controller, $G_e(s)$, from u_e to the extender position y_e is governed by position and velocity feedback gains. $G_p(s)$ and $G_d(s)$ are the transfer functions of the open-loop extender that show how the extender responds to the input current, i , and the forces, f_{en} and f_{eh} . The moment arm l_{eh} , representing the effect of the human force, is about one-third of l_{en} . The servo controller board, with a gain of K_b , outputs a current proportional to the command voltage, resulting in a displacement of the servovalve spool. The extender velocity is measured for feedback by a tachometer with a gain of K_t and is fed to the computer by an analog-to-digital convertor with a gain of K_{ad} . The extender position is measured by an encoder via a parallel IO board with a gain of K_{io} . The pre-compensator K_o is used as a constant gain to change the input units. K_1 and K_2 are position and velocity gains and K_{da} is the digital-to-analog convertor gain.

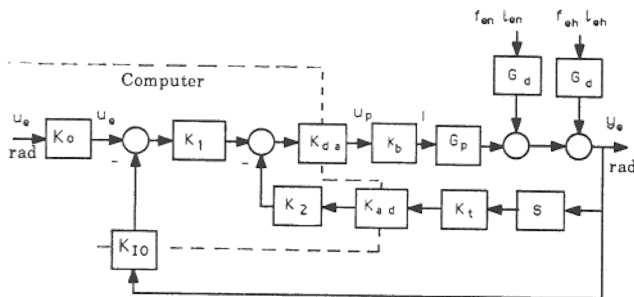


Figure 3: Block Diagram of the Closed-loop Position Controller, Tachometer gain: $K_t=0.169$ volts/(rad/sec), Servo controller board gain: $K_b= 0.00465$ ampere/volt, Digital to Analog Converter: $K_{da}=10$ volts/2048, Analog to Digital Converter: $K_{ad}=2048/1.25$ volts, Parallel IO gain: $K_{io}=1592$ number/rad, Pre-compensator gain: $K_o=1592$ number/rad, Position gain: $K_1=.94$, Velocity gain: $K_2=.00977$

Equations 37 and 38 are the experimentally verified transfer functions for G_p and G_d ⁴. Appendix A describes their detailed theoretical and experimental derivations.

$$G_p = \frac{y_e}{i} = \frac{355}{s(\frac{s^2}{1560.25} + \frac{s}{43.89} + 1)} \quad \text{rad/Ampere} \quad (37)$$

$$G_d = 135 \times 10^{-7} \frac{\frac{s}{23.6} + 1}{s(\frac{s^2}{1560.25} + \frac{s}{43.89} + 1)} \quad \text{rad/(lbf-inch)} \quad (38)$$

Using $K_1 = .94$ and $K_2 = 0.00977$ yields the widest bandwidth for the closed-loop transfer function, G_e , and guarantees the stability of the system in the presence of bounded unmodeled dynamics in the extender [7]. From Figure 3, an expression for G_e is derived in equation 39. Figure 4 depicts the theoretical and experimental values for the Bode plot of G_e .

$$G_e = \frac{y_e}{u_e} = \frac{1}{\frac{s^3}{18860} + \frac{s^2}{530.52} + \frac{s}{11.83} + 1} \quad \text{rad/rad} \quad (39)$$

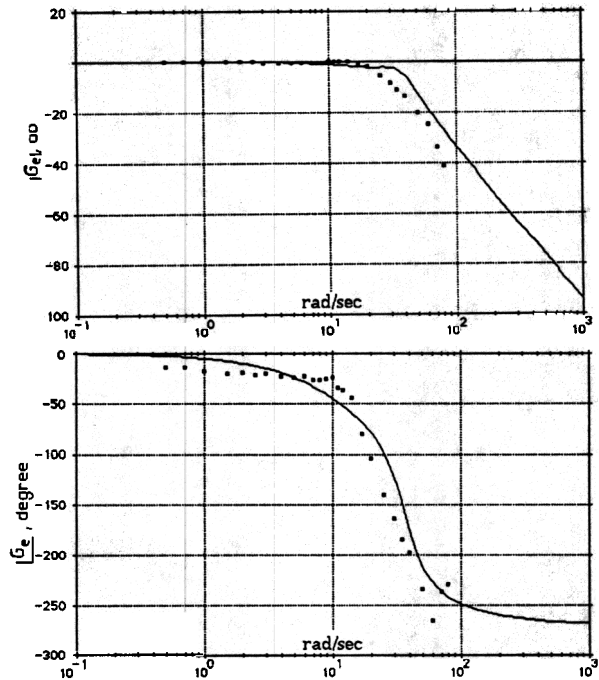


Figure 4: The Experimental and Theoretical Bode Plot of G_e . The extender position closed loop has the bandwidth of about 10 rad/sec.

S_{en} is defined as the sensitivity of the extender position y_e to f_{en} applied at a moment arm of $l_{en}=3'$. S_{eh} is defined as the sensitivity of the extender position to f_{eh} applied at a moment arm of $l_{eh}=1'$. By inspecting the block diagram of Figure 3 and substituting the parameter values, S_{en} can be found as follows:

$$S_{en} = \frac{y_e}{f_{en}} = 0.00004 \frac{\frac{s}{23.6} + 1}{\frac{s^3}{18860} + \frac{s^2}{530.52} + \frac{s}{11.83} + 1} \quad \text{rad/lbf} \quad (40)$$

Since the human arm force affects the extender about three times less than the environment force, S_{eh} is about three times less than S_{en} .

⁴ Hereafter, the arguments for all transfer functions will be omitted.

$$S_{eh} = \frac{L_{eh}}{L_{en}} S_{en} = 1.34 \times 10^{-5} \frac{\frac{s}{23.6} + 1}{\frac{s^3}{18860} + \frac{s^2}{530.52} + \frac{s}{11.83} + 1} \text{ rad/lbf}$$

10. ENVIRONMENT DYNAMIC ANALYSIS

An automobile strut, mounted on a custom fixture below the extender, is the experimental environment (Figure 1a). This environment can be modeled as a linear spring and damper system, where inertial effects of the strut are negligible compared to the spring and damping effects. The environmental stiffness and damping are measured to be 2050 lbf/rad and 200 lbf/(rad/sec) where radians represents the angular displacement of the motor shaft. A dynamic value for E_n is given in equation 42 where the bandwidth of 10 rad/sec can be observed.

$$E_n = 200s + 2050 \quad \text{lbf/rad} \quad (42)$$

11. HUMAN ARM DYNAMIC ANALYSIS

The model derived here does not represent human arm sensitivity, S_h , for all configurations; it is only an approximate and experimentally verified model of the author's elbow in the neighborhood of the Figure 1a configuration. The extender motion y_e in the case of this prototype, is a rotating motion about the elbow joint. If the human elbow behaves linearly in the neighborhood of the horizontal position, S_h is the human arm impedance. For the experiment, the author's elbow was placed in the extender, and the extender was commanded to oscillate via sinusoidal functions. In each frequency of the extender oscillation, the operator tried to move his hand and follow the extender so that zero contact force was created between his hand and the extender. Since the human arm cannot keep up with the high frequency motion of the extender when trying to create zero contact forces, large contact forces and consequently, a large S_h are expected at high frequencies. Since this force is equal to the product of the extender acceleration and human arm inertia (Newton's Second Law), at least a second-order transfer function is expected for S_h at high frequencies. On the other hand, at low frequencies (in particular at DC), since the operator can comfortably follow the extender motion, he can always establish almost zero contact forces between his hand and the extender. This leads to the assumption of a free derivative transfer function for S_h at low frequencies where contact forces are small for all values of extender position. Based on several experiments, at various frequencies, the best estimate for the author's hand sensitivity is presented by equation 43.

$$S_h = .143 s^2 + s \text{ lbf/rad} \quad (43)$$

Since, at low frequencies, particularly at DC, the human can usually create zero contact forces, equation 43 does not contain any nonzero DC gain. Figure 5 shows the experimental values and fitted transfer function for the human hand dynamic behavior.

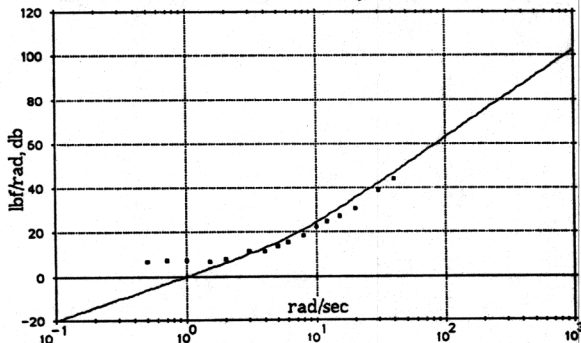


Figure 5: The Experimental and Theoretical Plot of S_h .

12. EXPERIMENTAL VERIFICATION OF STABILITY AND PERFORMANCE

The design objective is to decrease the force transferred to the human arm so the human feels the scaled-down values of the force imposed by the environment. This requires that $f_{eh} = -\alpha f_{en}$

where α is a scalar smaller than unity and represents the reduction of the force transmitted to the human arm. Using equations 15 and 16, H_1 and H_2 can be written as:

$$H_1 = \frac{2}{\alpha E_n G_e} \quad (44)$$

$$H_2 = \frac{1}{E_n G_e} \quad (45)$$

Substituting G_e and E_n from equations 39 and 42 into equations 44 and 45 gives H_1 and H_2 .

$$H_1 = \frac{2}{\alpha} \frac{\frac{s^3}{18860} + \frac{s^2}{530.52} + \frac{s}{11.83} + 1}{(200s + 2050)} \quad (46)$$

$$H_2 = \frac{1}{(200s + 2050)} \quad (47)$$

Equations 46 and 47 are improper transfer functions. For implementation on the computer, two high frequency poles are added to each of the transfer functions of equations 46 and 47⁵. The above values of H_1 and H_2 result in $f_{eh} = -\alpha f_{en}$. The designer cannot arbitrarily choose α ; in order to guarantee system stability, α must be chosen to guarantee inequality 34. However, if α is small (large force amplification), inequality 34 is violated at some frequencies, and no conclusion about stability can be made. Figure 6 depicting both sides of inequality 34 shows that for guaranteed stability of the closed-loop system, α must be larger than .143.

In the first set of experiments, α is chosen to be 0.5 to satisfy inequality 34, and it is shown that the closed-loop system is stable. The basic procedure for the experiment consisted of using the prototype extender to push on the fabricated environment in a series of periodic functions. The forces f_{eh} and f_{en} were measured and recorded in data files. The recorded f_{eh} was used as an input to a computer simulation encompassing the dynamic behavior of the extender, human, and environment. Figure 7 shows the simulated and experimental values of f_{en} along with the recorded value of f_{eh} for three different maneuvers when α is chosen to be 0.5 (twice force amplification). The experimental data and theoretical predictions are in close agreement. The first two plots are obtained using a low frequency human arm motion. This demonstrates the linearity between the input f_{eh} and the output f_{en} . Note that the output force f_{en} is consistently twice the input force f_{eh} . The second set of experiments was conducted with $\alpha = 0.03$, where the system exhibits instability in the form of oscillations (Figure 8). Inspection of Figure 6 shows that the choice of $\alpha = 0.03$ violates inequality 34. The trade-off between performance and stability can be observed here: the better the required performance (larger force amplification in this experiment), the narrower the stability range is. Since inequality 34 is only a sufficient condition for stability, violation of this condition does not lead to any conclusion. Figure 9 shows the experimental and simulated contact forces when $\alpha = 0.1$ (force amplified by a factor of 10). The system is stable and f_{en} is consistently ten times larger than the force f_{eh} , but the stability condition is not satisfied.

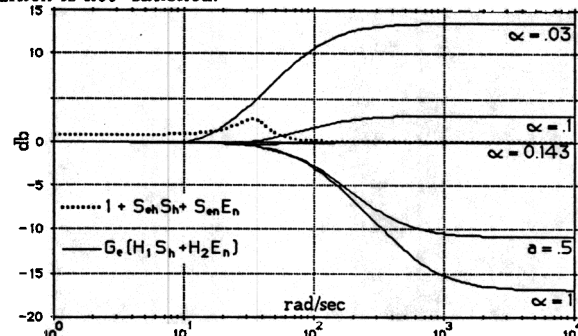


Figure 6: Inequality 34 (stability condition) is satisfied for $\alpha > .143$.

⁵ H_1 and H_2 are divided by the force sensor and the A/D convertor gains.

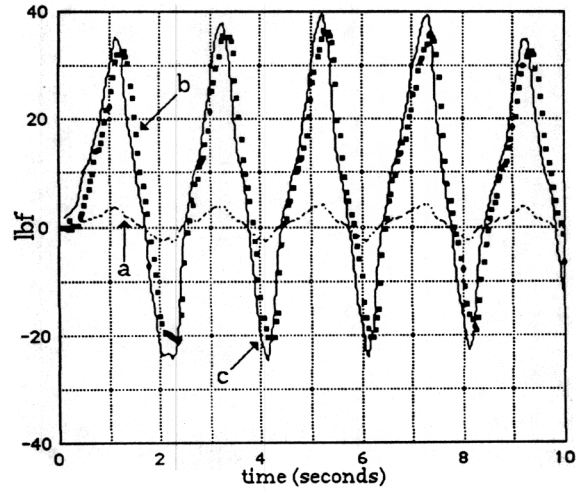
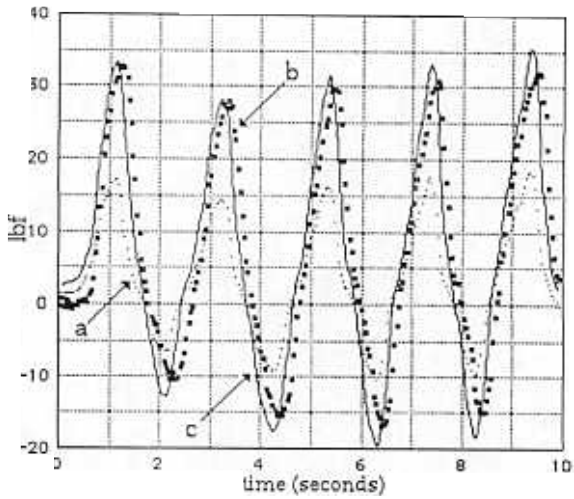
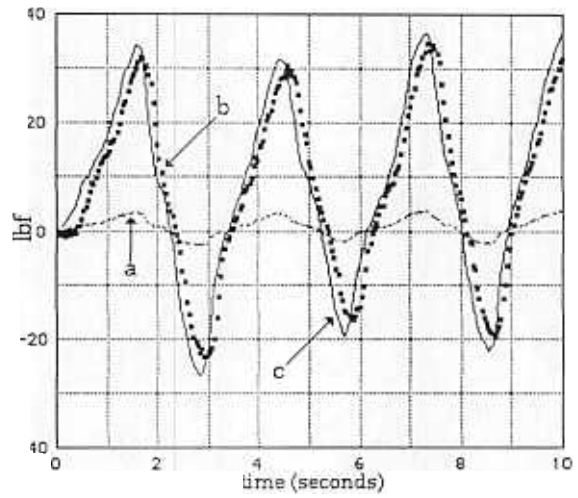
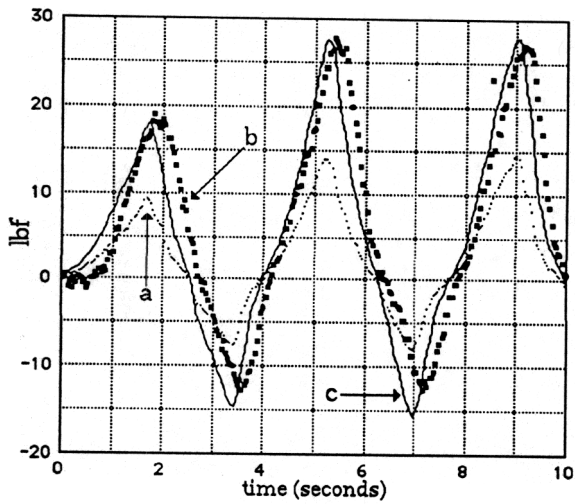
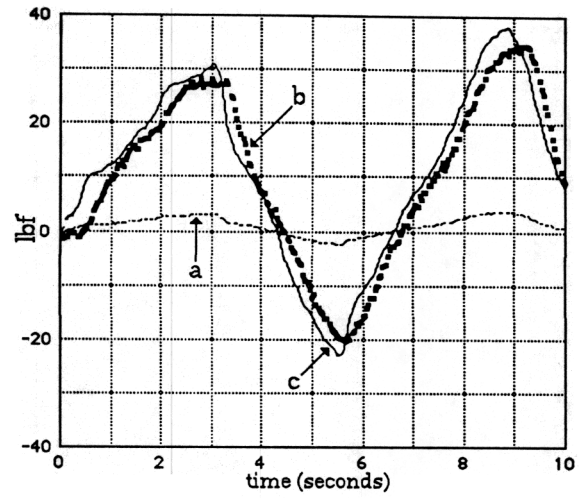
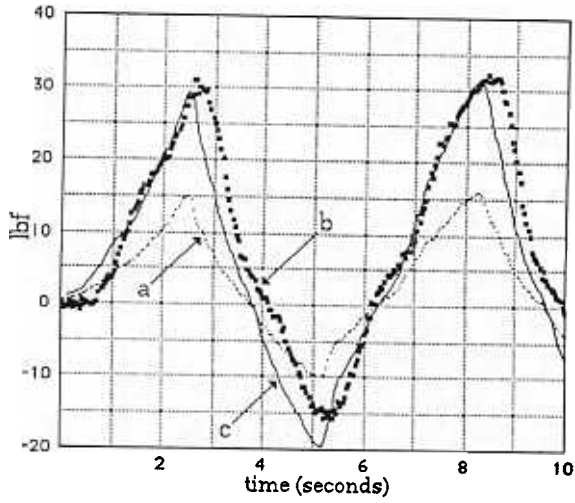


Figure 7: Stable maneuver with $\alpha=0.5$ (twice force amplification) a: f_{eh} , b: experimental f_{en} , c: simulated f_{en}

Figure 9: With $\alpha=1$ (ten times force amplification), H_1 and H_2 violate the stability condition; however, the system is stable.

a: f_{eh} , b: experimental f_{en} , c: simulated f_{en}

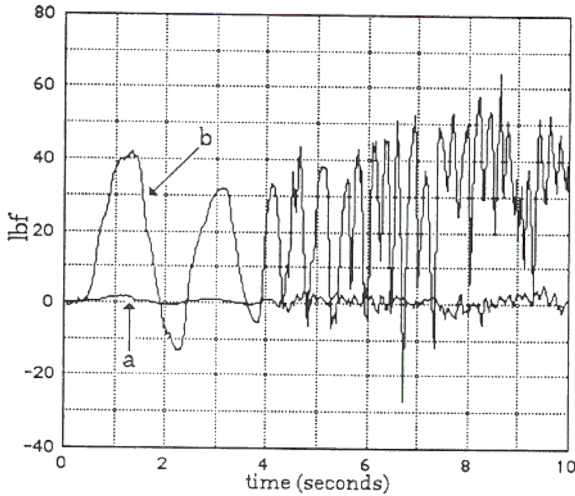


Figure 8: Unstable maneuver with $\alpha = .03$ (thirty times force amplification). H_1 and H_2 violate inequality 34, a: f_{eh} , b: experimental f_{en} .

13. SUMMARY AND CONCLUSION

This paper discusses the constrained motion in a class of human-controlled robotic manipulators called extenders. Extenders amplify the strength of the human operator, while utilizing the intelligence of the operator to spontaneously generate the command signal to the system. A single-degree-of-freedom extender has been built for theoretical and experimental verification of the extender dynamics and control. System performance is defined as amplification of human force. It is shown that the greater the required amplification, the smaller the stability range of the system is. A condition for stability of the closed-loop system (extender, human and environment) is derived, and, through both simulation and experimentation, the sufficiency of this condition is demonstrated.

APPENDIX A

Figure A1 shows the internal block diagram of the open-loop extender. The current, i , is the command input to the hydraulic servovalve which allows the flow of hydraulic fluid to the rotary actuator. f_{eh} and f_{en} are the forces imposed on the extender by the human and by the environment.

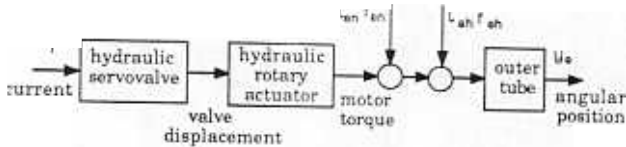


Figure A1: The Internal Block Diagram of G_p

The dynamics of the hydraulic servovalve and rotary actuator system are described by equations A1, A2, and A3 [13].

$$Q_1 = K_q i - K_p P_1 \quad (\text{valve equation}) \quad (A1)$$

$$Q_1 = \frac{d y_e}{dt} D_m + \frac{V_t}{4 \beta_e} \frac{d P_1}{dt} \quad (\text{flow continuity equation}) \quad (A2)$$

$$P_1 D_m + f_{en} l_{en} + f_{eh} l_{eh} = J \frac{d^2 y_e}{dt^2} \quad (\text{Newton's Law}) \quad (A3)$$

where f_{en} , l_{en} , f_{eh} , and l_{eh} are defined in Figure 1a and the other parameters are as follows:

- Q_1 load flow, in^3/sec
- K_a flow gain, $(\text{in}^3/\text{sec})/\text{amp}$
- current to drive servo valve, ampere
- K_p pressure gain, $\text{in}^5/(\text{sec lbf})$

- P_1 load pressure, psi
- y_e angular position of the extender, rad
- D_m actuator volumetric displacement, $7.62 \text{ in}^3/\text{rad}$
- J outer tube moment of inertia, $38.8 \text{ in-lbf-sec}^2$
- β_e hydraulic fluid modulus of elasticity
- V_t total contained volume in actuator, 13.3 in^3

Eliminating P_1 and Q_1 from equations A1, A2, and A3 gives Equation A4, a transfer function for the angular position of the open-loop extender, y_e .

$$y_e = G_p i + G_d f_{en} l_{en} + G_d f_{eh} l_{eh} \quad (A4)$$

where:

$$G_p = \frac{K_q}{D_m} \frac{1}{s \left(\frac{s^2}{\omega_e^2} + \frac{2 \zeta_e s}{\omega_e} + 1 \right)}, \quad G_d = \frac{K_p}{D_m^2} \frac{\frac{V_t s}{4 \beta_e K_p} + 1}{s \left(\frac{s^2}{\omega_e^2} + \frac{2 \zeta_e s}{\omega_e} + 1 \right)}$$

and

$$\omega_e = D_m \sqrt{\frac{4 \beta_e}{V_t J}}, \quad \zeta_e = \frac{K_p}{D_m} \sqrt{\frac{\beta_e J}{V_t}}$$

By fitting G_p into an experimentally-derived Bode plot (Figure A2), the following parameters are derived:

$$\frac{K_q}{D_m} = 355 \text{ (rad/sec)/amp,}$$

$$\omega_e = 39.5 \text{ rad/sec}$$

$$\zeta_e = 0.45$$

Using the above data, G_p is given by equation A5.

$$G_p = \frac{355}{s \left(\frac{s^2}{1560.25} + \frac{s}{43.89} + 1 \right)} \text{ rad/amp} \quad (A5)$$

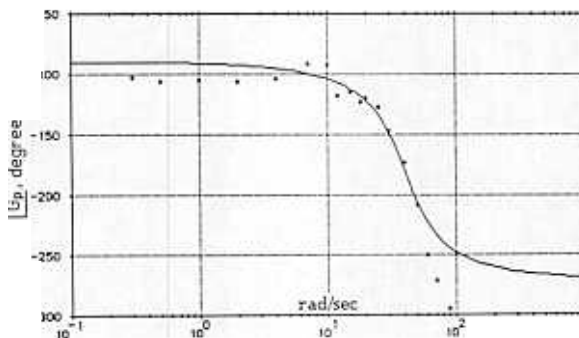
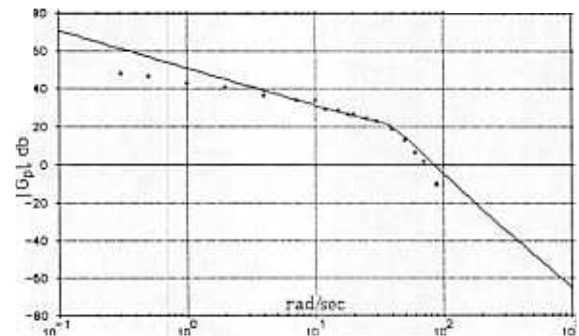


Figure A2: Experimental Data and Theoretical G_p .

$\frac{K_p}{D_m^2}$ was determined to be 135×10^{-7} (rad/sec)/(lbf·inch).

Using the values stated for V_t , β_e , and D_m , the numerical value for G_d is given by expression A6.

$$G_d = 135 \times 10^{-7} \frac{\frac{s}{23.6} + 1}{s^2 + 1} \text{ rad/(lbf·inch)} \quad (A6)$$

REFERENCES

- 1) Clark, D.C. et al., "Exploratory Investigation of the Man-Amplifier Concept", U.S. Air Force AMRL-TDR-62-89, AD-390070, August 1962.
- 2) GE Company, "Exoskeleton Prototype Project, Final Report on Phase I", Report S-67-1011, Schenectady, NY, 66.
- 3) GE Company, "Hardiman I Prototype Project, Special Interim Study", Report S-68-1060, Schenectady, NY, 1968.
- 4) Groshaw, P. F., "Hardiman I Arm Test, Hardiman I Prototype", Report S-70-1019, GE Company, Schenectady, NY, 1969.
- 5) Hollerbach, J.M., "A Recursive Lagrangian Formulation of Manipulator Dynamics and a Comparative Study of Dynamics Formulation Complexity", IEEE Trans. on Systems, Man and Cybernetics Vo. 10, No. 11, pp. 730-736, Nov., 1980.
- 6) Kazerooni, H., "Human Machine Interaction via the Transfer of Power and Information Signals", IEEE International Conference on Robotics and Automation, May 1989, Scottsdale, Arizona, pp. 1632-1642.
- 7) Kazerooni, H., "Loop Shaping Design Related to LQG/LTR for SISO Minimum Phase Plants", International Journal of Control, Volume 48, Number 1, July 1988.
- 8) Kazerooni, H., Tsay, T. I., "Stability Criteria for Robot Compliant Maneuvers", In proceeding of the IEEE International Conference on Robotics and Automation, Philadelphia, PA, April 1988.
- 9) Kazerooni, H. "Design and Analysis of the Statically Balanced Direct Drive Manipulator", IEEE Control System Magazine, Volume 9, Number 2, February 1989.
- 10) Kazerooni, H., Sheridan, T. B., Houpt, P. K., "Robust Compliant Motion for Manipulators", IEEE J. of Robotics and Automation, Vo. 2, No. 2, June 1986.
- 11) Lehtomaki, N.A., Sandell, N.R., Athans, M., "Robustness Results in Linear-Quadratic Gaussian Based Multivariable Control Designs", IEEE Trans. on Auto. Control, Vol. AC-26, No. 1, pp. 75-92, February 1981.
- 12) Makinson, B. J., "Research and Development Prototype for Machine Augmentation of Human Strength and Endurance, Hardiman I Project", Report S-71-1056, General Electric Company, Schenectady, NY, 1971.
- 13) Merritt, H. E., "Hydraulic Control Systems", John Wiley & Sons, Inc., 1967.
- 14) Mizen, N. J., "Preliminary Design for the Shoulders and Arms of a Powered, Exoskeletal Structure", Cornell Aeronautical Laboratory Report VO-1692-V-4, 1965.
- 15) Mosher, R.S., "Force Reflecting Electrohydraulic Servomanipulator", Electro-Technology, pp. 138, Dec. 60.
- 16) Mosher, R. S., "Handyman to Hardiman", SAE Report 670088.
- 17) Vidyasagar, M., "Nonlinear Systems Analysis", Prentice-Hall, 1978.